Mayor, J., Bora, S. S., Cotton, F. (2018): Capturing Regional Variations of Hard-Rock κ0 from Coda Analysis. - *Bulletin of the Seismological Society of America*, *108*, 1, pp. 399—408.

DOI: http://doi.org/10.1785/0120170153

Capturing Regional Variations of Hard-Rock κ_0 from Coda Analysis

by Jessie Mayor*, Sanjay Singh Bora†, and Fabrice Cotton‡

Abstract We propose an alternative procedure for the capture of the hard-rock regional kappa ($\kappa_{0_{ref}}$). In our approach, we make use of a potential link between the well-known κ parameter and the properties of coda waves. In our analysis, we consider near-distance records of four crustal earthquakes of local magnitude 3.7–4.9 that occurred in four regions of France in different geological contexts: the crystalline axial chain of Pyrenees to the southwest, the large sedimentary basin to the southeast, the Alpine range to the east, and the extensional Rhine graben to the northeast. Each earthquake has been recorded at a pair of nearby soft- and hard-rock station sites. The high-frequency (16–32 Hz) spectral amplitudes of the coda window (carefully selected on the time series of the accelerograms) confirm an exponential decrease, which we quantify by $\kappa_{AH_{coda}}$ and call "kappa of coda." It is found that $\kappa_{AH_{coda}}$ is independent of the soil type but shows significant regional variations. κ measurements (*Anderson and Hough*, 1984) over the coda window ($\kappa_{AH_{coda}}$) and full time series (κ_{AH}) show strong correlation at hard-rock sites. This suggests that $\kappa_{AH_{coda}}$ can provide a new proxy to estimate the regional hard rock $\kappa_{0_{ref}}$ (*Ktenidou et al.*, 2015). Theoretical analysis is also presented to relate the regional $\kappa_{AH_{coda}}$ and coda quality factor Q_c, which quantifies the average attenuation properties of the crust (both scattering and absorption). It allows interpreting $\kappa_{AH_{coda}}$ as the time spent by the waves in the medium, weighted by its attenuation properties. This theoretical analysis also shows that the classical κ measurement should be frequency dependent; this was confirmed by the spectra of the observed records.

Introduction

Parameterization of high-frequency ground motions beyond source-corner frequency (*Brune*, 1970, 1971) has received significant attention in last few decades (e.g., *Hanks*, 1982; *Anderson and Hough*, 1984). κ (kappa), an empirical parameter, introduced by *Anderson and Hough* (1984), is often used to represent the spectral decay of acceleration spectrum $A(f)$at high frequencies ($f > 10$ Hz). This is done using a simple exponential filter, as follows:

$$A(f) \propto \exp(-\pi f). \tag{1}$$

Owing to its strong impact on hazard calculations (*Molkenthin et al.*, 2017), κ has been widely used in stochastic simulation of ground motion (*Boore*, 2003) and in the host-to-target adjustments (HTTA) of empirical ground-motion prediction equations (GMPEs; e.g., *Campbell*, 2003; *Cotton et al.*, 2006; *Zandieh et al.*, 2016). Recently, κ has been used in the GMPEs itself as one of the predictor variables (*Bora et al.*, 2015). This high-frequency (empirical) attenuation parameter is one of the most used and yet least understood (or agreed upon) parameters in engineering seismology. Moreover, the physical mechanism causing the observed fall-off in acceleration spec-

* Now at EDF-Lab Paris-Saclay, 7 Boulevard Gaspard Monge, 91120 Palaiseau, France.
† Now at Swiss Seismological Service (SED), ETH Zurich, Sonneggstrasse 5, NO H 60, 8092 Zurich, Switzerland.
‡ Also at Institute for Earth and Environmental Sciences, University of Potsdam, 14469 Potsdam, Germany.

trum at high frequencies is heavily debated in literature (we refer the reader to *Ktenidou et al.*, 2014, for a detailed review).

Anderson (1991) suggested a preliminary model for κ that includes contributions from path (κ_r) and site (κ_0) effects as follows:

$$\kappa = \kappa_0 + \kappa_r R, \tag{2}$$

in which R represents distance (epicentral or hypocentral). *Kilb et al.* (2012) found that a source component can also be present that essentially increases the variability of the κ_0 estimate. However, in this article, we focus our discussion on the site κ_0.

Recently, *Ktenidou et al.* (2015) observed that κ_0 stabilizes for high V_{S30} values (time-averaged shear-wave velocity at a point located 30 m beneath the station), which may indicate the existence of regional hard-rock effects in κ_0. They proposed that this hard-rock κ_0 essentially determines the nature of the crust in the region. The existence of such regional dependency of hard-rock κ_0 has strong implications for site-specific hazard assessment. Indeed, the common practice for site-specific ground-motion prediction requires not only the properties of the soil layers (e.g., shear-wave velocities) but also κ_0 of the base-rock layer (*Rodriguez-Marek et al.*, 2014). The lack of hard-rock records and the poor understanding of the physics of kappa introduced significant epistemic uncertainty in the final seismic hazard of recent projects (*Renault*, 2014; *Edwards et al.*, 2015). Thus, determining precise and accurate regional hard-rock κ_0 values is critical to reduce uncertainty in rock-reference seismic hazard.

Following *Ktenidou et al.* (2015) and using a notation scheme suggested by *Edwards et al.* (2013), κ_0 contains (1) the upper local site effect ($\Delta\kappa$) caused by the shallow sedimentary layers beneath the receiver and (2) $\kappa_{0_{ref}}$ related to the regional (reference) hard-rock attenuation effect as follows:

$$\kappa_0 = \kappa_{0_{ref}} + \Delta\kappa. \tag{3}$$

Although it is relatively easy to estimate κ and κ_0 from data, as shown by many authors (*Van-Houtte et al.*, 2011; *Kilb et al.*, 2012; *Ktenidou et al.*, 2012; *Lai et al.*, 2016; *Bora et al.*, 2017), one of the major challenges that remains is to distinguish between the two separate contributions of $\kappa_{0_{ref}}$ and $\Delta\kappa$. Capturing the regional effect in κ_0 is difficult to achieve because surface hard-rock stations are rare. It has thus been suggested that borehole measurements may be useful in determining these values, at the expense of high cost procedures (*Ktenidou et al.*, 2015).

In this article, we propose another technique to estimate $\kappa_{0_{ref}}$, using the multiple scattered coda waves. Coda waves have been widely used to characterize the seismic attenuation of the crust (*Carcolé and Sato*, 2010; *Calvet et al.*, 2013; *Mayor et al.*, 2016, 2017; *Sedaghati and Pezeshk*, 2016) from the analysis of the coda quality factor Q_c that quantifies the energy (E) decay of coda waves as a function of time t as follows:

$$E(t, f_m) \propto \exp\left\{-\frac{2\pi f_m t}{Q_c(f_m)}\right\} \times t^{-\alpha}, \tag{4}$$

in which f_m is the central frequency of the band-pass-filtered time series, and α a fixed exponent that depends on the interpretative model of coda wave propagation (see *Sato et al.*, 2012, for details). Ever since the pioneering work of *Aki and Chouet* (1975), who parameterized equation (4), it has been observed worldwide that (1) Q_c is strongly frequency dependent; Q_c increases with frequency as reported in the literature by *Aki and Chouet* (1975), *Steensma and*

Biswas (1988), *Leary and Abercrombie* (1994), and *Paul et al.* (2003), among others. Additionally, it has been observed that (2) Q_c is insensitive to the source and site effects (*Aki and Chouet*, 1975; *Rautian and Khalturin*, 1978; *Lacombe et al.*, 2003; *Sato and Fehler*, 2007). This knowledge is essential when characterizing the propagation properties of the crust. We thus propose a new technique to retrieve the hard-rock κ_0 of our four main French regions by performing the classical κ measurement given by *Anderson and Hough* (1984) on the coda spectrum. This will be done in a fixed 16–32 Hz high-frequency band that we call "kappa of coda," represented by the notation $\kappa_{AH_{coda}}$. The octave band (16–32 Hz) is arbitrarily fixed because (1) it quantifies the overall high-frequency decrease of the Fourier spectra up to the noise level, and (2) it has been used in coda analyses over the four regions of this study (*Mayor et al.*, 2017). These analyses will be used later in this article for comparative purpose.

Hereafter, $\kappa_{AH_{coda}}$ and κ_{AH} will be used to represent classical κ measurements over coda and full time-series windows, respectively. The analysis presented in this article is unique in the sense that it connects a typical engineering measure of attenuation to a classical seismological concept of attenuation. Thus, it provides an alternative perspective on the whole kappa issue that is widely debated in the literature.

After describing the data explored in this study, the next sections will show that $\kappa_{AH_{coda}}$ values are (1) independent of the site conditions and strongly dependent on the region under study (the Site Independence and Regional Variations of $\kappa_{AH_{coda}}$ section) and (2) $\kappa_{AH_{coda}}$ could be related to the hardrock $\kappa_{0_{ref}}$ (the $\kappa_{AH_{coda}}$ and Hard-Rock κ_0 section). We finally show that $\kappa_{AH_{coda}}$ is related to the well-known coda quality factor Q_c (equation 3), which implies a frequency dependence of $\kappa_{0_{ref}}$ and a fortiori of κ_{AH}.

Data and Processing

The present analysis, of which the first goal is to estimate $\kappa_{AH_{coda}}$, is strictly performed on the coda part of the signal that was recorded in Metropolitan France. As the studied area is characterized by low-to-moderate seismicity, the selected earthquakes need to have a fairly large magnitude (criterion 1) compared to the classical magnitudes observed in the region. In this way, the records should exhibit a rather good signal-to-noise ratio (typically higher than 4), especially in the coda window. The second objective of the present work is to compare the effects of the soil conditions on the $\kappa_{AH_{coda}}$ values. This implies that we need to select only earthquakes that have been recorded over the same distance range and within the same area, by a pair of stations located on rock and soil sites (criterion 2). The two criteria considered above lead to the selection of a limited number of earthquakes. For that reason, the present analysis is performed on acceleration recordings made from only four crustal earthquakes, namely the 26 February 2005 SSE St. Béat, the 25 February 2001 SSE Nice, the 30 June 2010 St. Jean-deMaurienne, and the 5 December 2004 Waldkirch; these have magnitudes ranging from 3.7 to 4.9 (Bureau Central Sismologique Français). These earthquakes have been recorded on the three components (Z for vertical, E for east–west, and N for north–south) in four different French geological regions: (1) the crystalline axial chain of Pyrenees in the southwestern part, (2) the sedimentary southeast basin in the extreme southeastern part of France, (3) the back-arc region of the Alps in the southeast, and (4) the Rhine graben region in northeastern France. These four earthquakes are located in areas where regional variations of Q_c have been recently mapped by *Mayor et al.* (2017). As required by our analysis, each of the earthquakes has been recorded at a pair of soft- and hard-rock station sites. The sites were carefully selected using the site-response analysis of *Drouet et al.* (2010) for the French accelerometric network. Indeed, we choose stations with well-constrained amplification factors close to 1 and greater for hard-rock and soft-soil sites, respectively. The 24 selected accelerograms (8 source-station pairs with 3 component recordings) were downloaded from the RESIF (French seismologic and geodetic network) data center and subsequently corrected using instrumental response. It is worth mentioning here that we select only near-distance records to minimize the bias in κ_0 that can occur due to path-

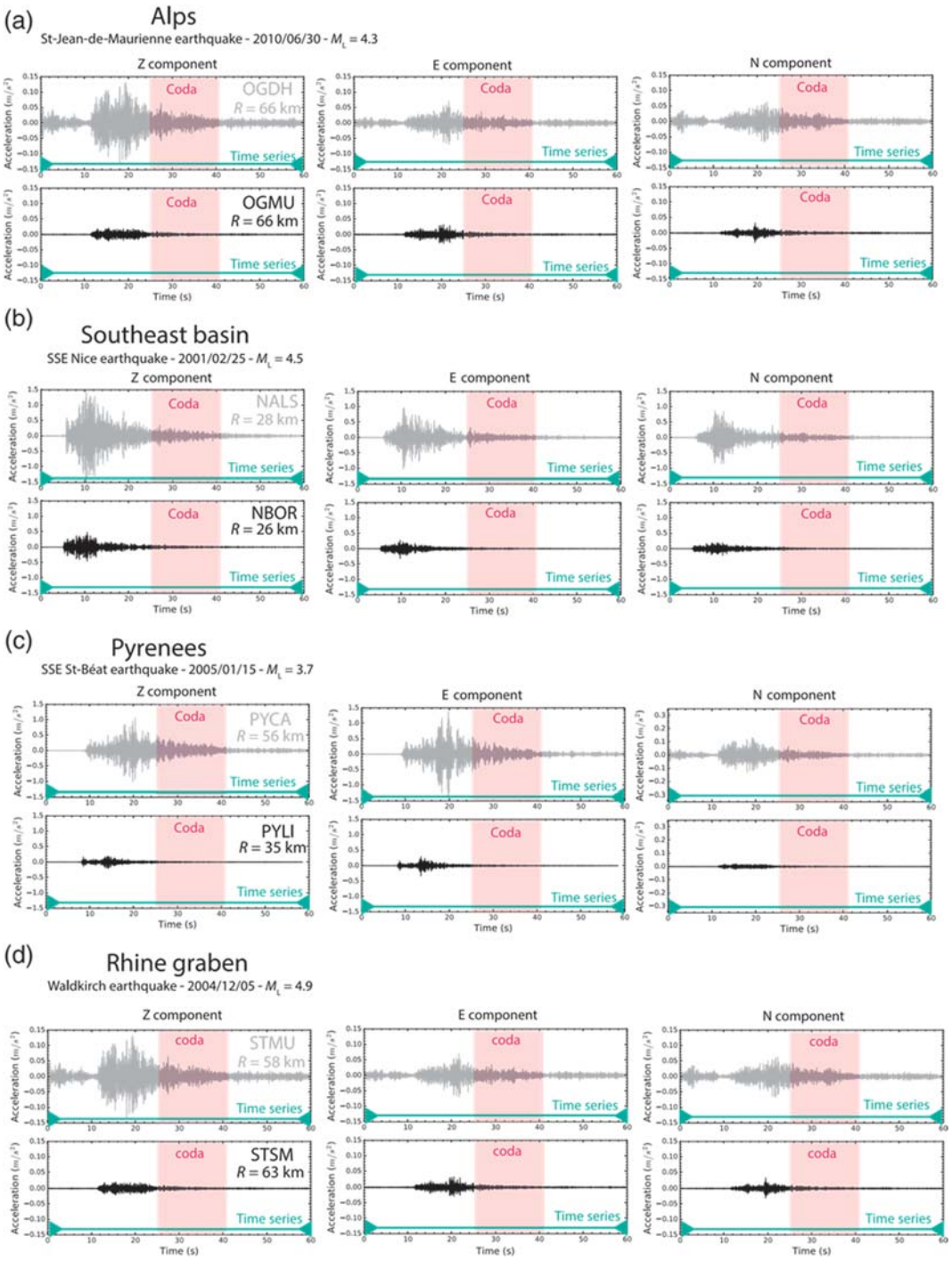

Figure 1. *Three components (Z, vertical; E, east–west; and N, north–south) of the 24 accelerograms (filtered in the 16–32 Hz frequency band) used in this study. For each of the four explored regions, a record from a soft-soil site (gray) and from a hard-rock station (black) have been analyzed. The details about the four earthquakes (date and magnitude) are mentioned under each region. The station name and the epicentral distance R are indicated on the top-right corner of each record. The coda window of onset time $t_w = 25$ s and duration $L_w = 15$ s is pointed out by the rectangle. The bottom line along the x axis shows the length of the full time series used for the κ_{AH} measurement.*

related attenuation (Q). The epicentral distance ranges from 26 to 66 km. Furthermore, keeping in mind that our analysis is focused on high-frequency attenuation, each of the acceleration traces was band-pass filtered in the 16–32 Hz frequency band. We analyze full (filtered) time series, as well the time series for a selected coda window. As can be seen in Figure 1, we define a coda window with an onset time $t_w = 25$ s from the origin time

with a duration of $L_w = 15$ s. Depending on the set of epicentral distances that we have, the parameters t_w and L_w may be different but carefully chosen; the reader can refer to the work of *Calvet and Margerin* (2013) to select the best coda window. We also ensure in our processing that the signal-to-noise ratio is greater than four for the whole coda, as expected. Indeed, we define the noise level as the average of the squared acceleration within a window of 5 s starting at the beginning of the record. We subsequently verify that the average acceleration on the coda window ($t = 25$ s until 40 s, see the rectangle in Fig. 1) is greater than 4. A clear difference can be observed in accelerograms recorded at soft-soil and hard-rock stations in terms of both amplitude and duration (Fig. 1).

κ_{AH} and $\kappa_{AH_{coda}}$ Measurements

As stated in the Introduction, we make κ measurements of *Anderson and Hough* (1984) on full time series as well as on the coda window. It is worth mentioning here that we measure κ_{AH} and $\kappa_{AH_{coda}}$ in the 16–32 Hz frequency band, which is different from what is done in the original method of *Anderson and Hough* (1984). Indeed, authors usually prefer to visually inspect the frequency band where the linear decrease is clear in the linear–log plot of Fourier amplitude spectra (FAS). As we mention in the Introduction, here we choose a fixed frequency band because (1) it quantifies the overall high-frequency decrease of the Fourier spectra until the noise level and (2) it has been explored in coda analysis over the four regions of this study (*Mayor et al.*, 2017) which will be used for comparison in the Site Independence and Regional Variations of $\kappa_{AH_{coda}}$ section.

To estimate κ_{AH} over the full time series, linear regression on the Fourier spectral amplitudes as a function of frequency was performed; this is depicted in the top panels (of each region) in Figure 2. Finally, the slope of the best-fit line was corrected using equation (1) to obtain κ_{AH} for each time series. Similarly, the $\kappa_{AH_{coda}}$ was also estimated from FAS of the coda windows, as can be seen in the bottom panels (of each region) in Figure 2. A moving-average window of length 0.1 Hz was applied to smooth the coda spectrum; because of that, a larger correlation coefficient for the linear regression was obtained.

Site Independence and Regional Variations of $\kappa_{AH_{coda}}$

It can be observed from Figure 2 that, irrespective of the soil type and the part of the accelerograms (full or coda) used, there is a large variation (~70%) in high-frequency attenuation between the southeast basin and the Rhine graben. This observation indicates strong lateral variations in attenuation properties of the crust, as also observed by *Drouet et al.* (2010) and mapped by *Mayor et al.* (2017). In this context, two important observations can be made from Figure 2: (1) The kappa measurements and mainly $\kappa_{AH_{coda}}$ show little variations (maximum 20%) between the soil types, whereas (2) the $\kappa_{AH_{coda}}$ measurements are seen to vary regionally. Indeed, the effect of soil type is mainly seen in spectral level and not in the slope of the frequency decay. To validate our observations further, we superimpose our $\kappa_{AH_{coda}}$ measurements for each of the eight stations over the regional Q_c (16–32 Hz) map of *Mayor et al.* (2017) in Figure 3. Only Z-components are used for this comparison because *Mayor et al.* (2017) only used the Z-component for their mapping procedure. In Figure 3, soft-soil and hard-rock station sites are distinguishable by white and black contoured lines around the colored triangles, respectively. Interestingly, regional variations are clear in $\kappa_{AH_{coda}}$ and correlate well with the Q_c map of *Mayor et al.* (2017), whereas the $\kappa_{AH_{coda}}$ values are rather insensitive to the soil type. Our $\kappa_{AH_{coda}}$ values decrease from the Rhine graben, Alps, Pyrenees, and southeast basin with increasing regional Q_c values.

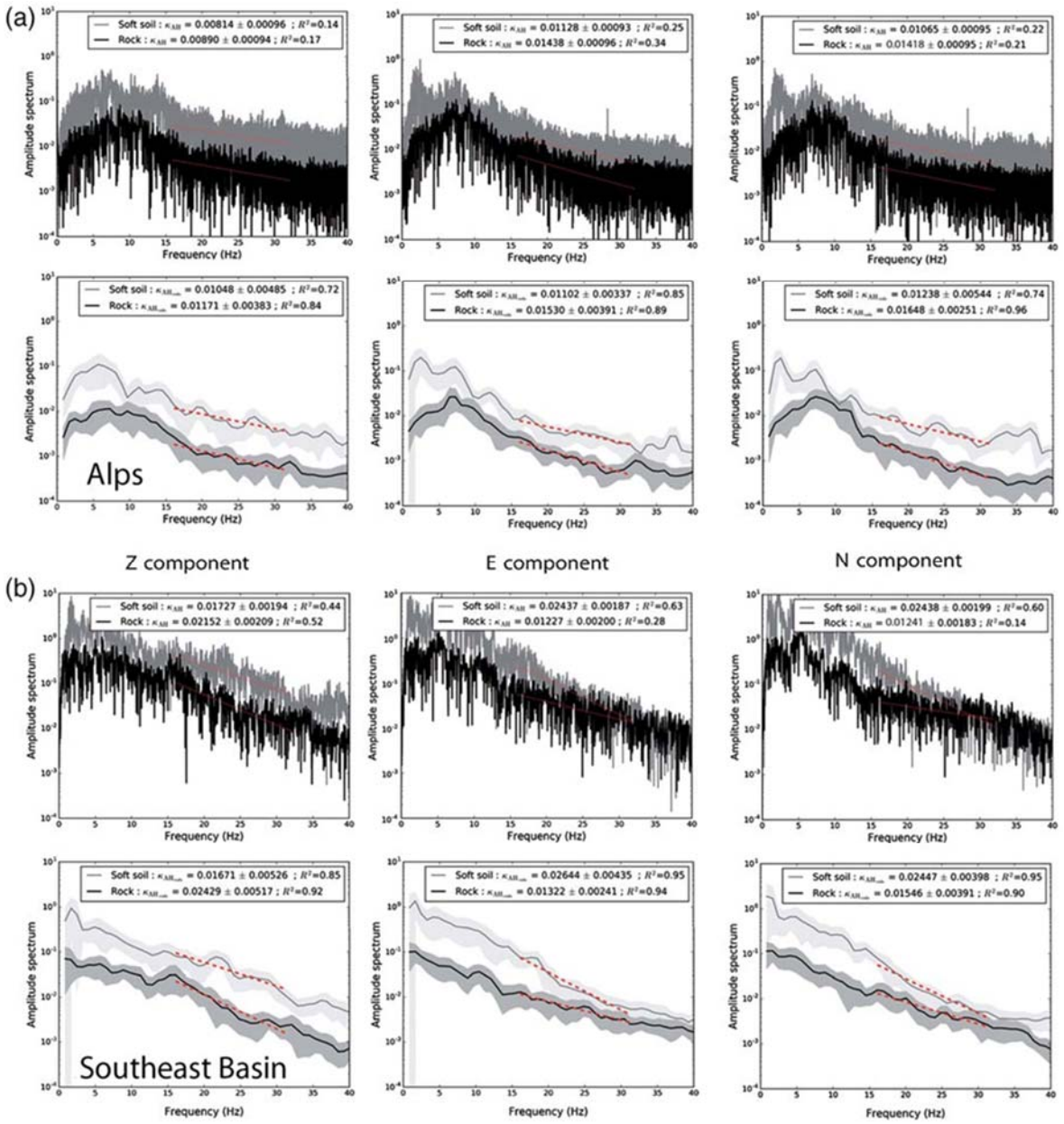

Figure 2. *Fourier amplitude spectra (FAS) of the whole time series (upper line) and the coda time series (lower line) in each of the four regions considered in this study: (a) Alps, (b) southeast basin, (c) Pyrenees, and (d) Rhine graben. The corresponding linear fit in the 16–32 Hz frequency band is shown by the dotted line. κ_{AH}, $\kappa_{AH_{coda}}$, and the corresponding correlation coefficient of the linear regression are indicated in the text box shown in each plot.* *(Continued)*

$\kappa_{AH_{coda}}$ and Hard-Rock κ_0

Ktenidou et al. (2015) proposed that κ_0 (equation 3) is described by three properties: (1) κ_0 is a site term and thus independent of source-to-site distance, (2) κ_0 is dependent upon the site amplification, and (3) κ_0 is composed of deeper effects, namely hard-rock $\kappa_{0_{ref}}$. Our $\kappa_{AH_{coda}}$ values that were obtained from the coda spectrum satisfy item 1; for instance, the estimates of $\kappa_{AH_{coda}}$ in Pyrenees performed at $R = 35$ and 56 km are independent of soil type as well as of the source-to-site distance effect. Physically, coda waves are strongly sensitive to the properties of the crust within a radius of 0.25ℓ (with ℓ being the scattering mean free path of the order of 100 km for the standard crust) around the source and the station, when the time in the coda is equal to twice

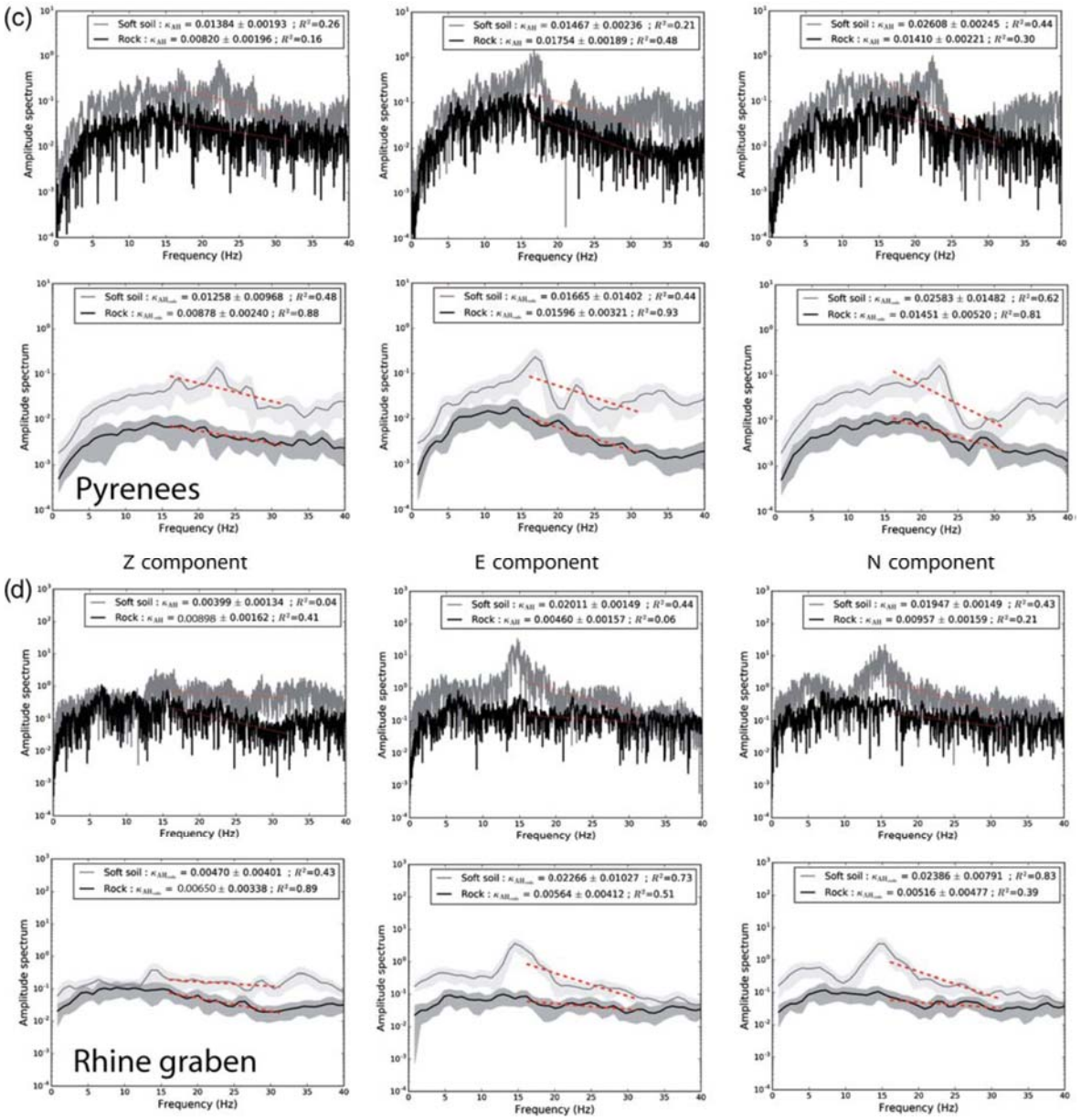

Figure 2. *Continued.*

the time of the S wave (*Mayor et al.*, 2014). Regarding our epicentral distance range (~50 km in average) and the location of our coda window ($t_w = 2t_S$), we can infer that coda waves tend to average the properties of the crust in the volume containing the source and receiver. Considering the near-distance earthquakes in our analysis (with a limited distance range of 26–66 km), we expect that the coda wave-train samples will contain almost the same volume of the crust in each region of investigation. Item 2 pointed out by *Ktenidou et al.* (2015) is not observed in our $\kappa_{AH_{coda}}$ estimates, as discussed in the Site Independence and Regional Variations of $\kappa_{AH_{coda}}$ section (in Figs. 2 and 3). This suggests that $\kappa_{AH_{coda}}$ is not linked with $\Delta\kappa$ (equation 3) and not affected by surficial layers beneath the station. However, $\kappa_{AH_{coda}}$ indicates regional variations, (Fig. 3) as expected by *Ktenidou et al.* (2015) for $\kappa_{0_{ref}}$ (κ measured at a hard-rock station from the full time series, i.e., κ_{AH}). To further explore this potential link between $\kappa_{0_{ref}}$ and $\kappa_{AH_{coda}}$, we show in Figure 4 the $\kappa_{AH_{coda}}$ values against corresponding κ_{AH} values for the four hard-rock stations used in our analysis. A clear and strong correlation can be observed between

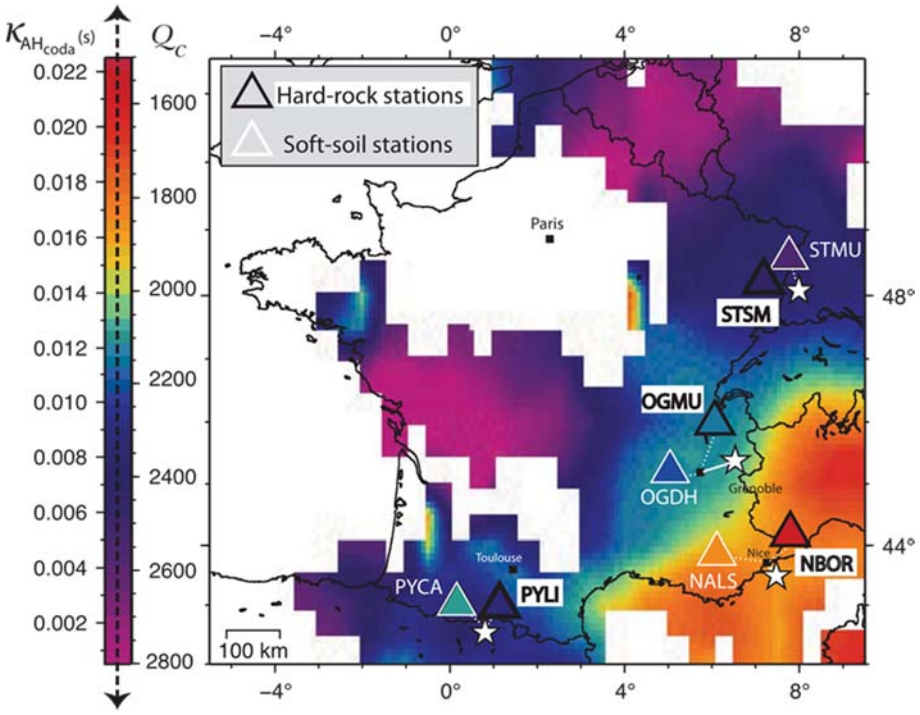

Figure 3. *$\kappa_{AH_{coda}}$ of the Z-component estimated for each source (white star) and station (triangle) pairs is reported (left color scale). The Q_c map performed with a Z-component dataset of the 16–32 Hz frequency band of Mayor et al. (2017) is also depicted (right color scale). Soft-soil and hard-rock stations are outlined with white and black triangles, respectively.*

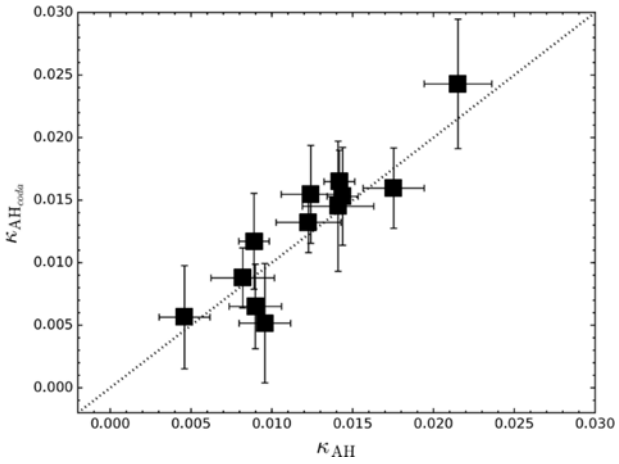

Figure 4. *Estimates of $\kappa_{AH_{coda}}$ against κ_{AH} measured in the 16–32 Hz frequency band at hard-rock sites in the four regions considered in this study.*

the two κ estimates. This observation suggests that $\kappa_{AH_{coda}}$ can potentially capture the regional hard-rock $\kappa_{0_{ref}}$, as pointed out by *Ktenidou et al.* (2015). Because $\kappa_{AH_{coda}}$ is measured over the coda part of the full time series, we postulate that it can be related to the well-known classical Q_c (*Aki and Chouet*, 1975), which will be discussed in the Frequency Dependence of $\kappa_{AH_{coda}}$ and κ_{AH} section.

Frequency Dependence of $\kappa_{AH_{coda}}$ and κ_{AH}

As shown in Figure 3, our estimates of $\kappa_{AH_{coda}}$ are rather free from soil-type effects and mimic the regional variations of Q_c. With the help of equation (4), it can be theoretically proven that the $\kappa_{AH_{coda}}$ measured according to our approach is related to Q_c by the following equation:

$$\kappa_{AH_{coda}}(f) = \frac{\tau}{Q_c(f)}, \tag{5}$$

in which τ is the central time of the coda window, starting from the origin time of the earthquake (in our case, $\tau = 32$ s). A physical interpretation of equation (5) can be that it describes $\kappa_{AH_{coda}}$ as a weighted time (weighted by attenuation properties quantified by Q_c) spent by the wave in the crust. The attenuation could be due to

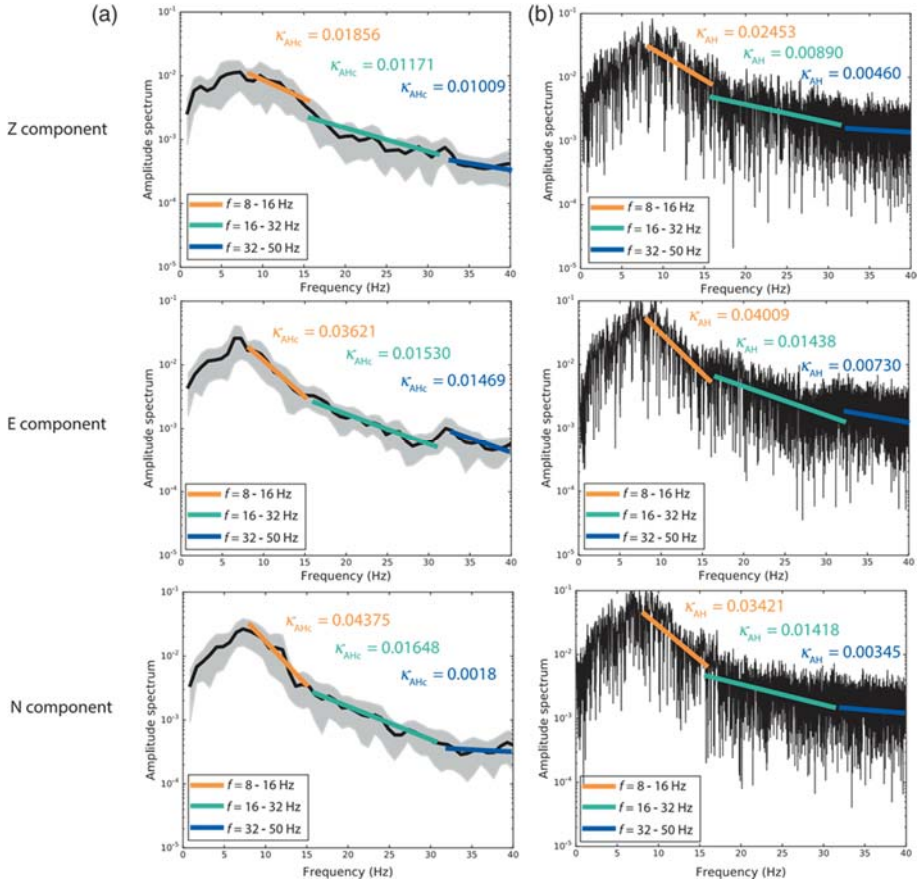

Figure 5. *FAS of (a) coda window and (b) full time series. The thick colored lines correspond to the linear fit in each frequency band depicted in the legend.*

absorption and scattering processes. In this study, the relationship shown in equation (5) is observed with a standard deviation of not more than 30%. Indeed, we estimated Q_c for each of the hard-rock records following the standard *Aki and Chouet* (1975) procedure that was detailed in *Mayor et al.* (2016); this was done in the 16–32 Hz band. We fixed $\alpha = 3/2$ in equation (4) to interpret coda waves as multiple scattered waves (see *Aki and Chouet*, 1975, for details). We found that Q_c is equal to 2308, 2069, 1881, and 1629 from the Z-component for the Rhine graben, Alps, Pyrenees, and southeast basin, respectively, as illustrated in Figure 3. We subsequently applied equation (5) to obtain the theoretical estimates of $\kappa_{AH_{coda}}$. We consider that the 30% between the predicted and the estimated values of $\kappa_{AH_{coda}}$ is an acceptable figure, given that the uncertainties of Q_c and $\kappa_{AH_{coda}}$ are both on the order of 20%. Our rationale regarding this small variability is that we are very strict (1) in our choice of data both in station and earthquake selections and (2) in our data processing. We are aware that further studies need to be performed with a larger data set to be able to statistically quantify the variability in the measurement of $\kappa_{AH_{coda}}$. We also note that the Rhine graben hard-rock record is a unique case because the Q_c value is measured close to the S wave. This implies that Q_c is not completely free from scattering and anisotropy effects (see *Aki and Chouet*, 1975, for a complete review on the measurement of Q_c and its physical interpretation according to the location of the coda window), which allows us to explain a stronger difference between predicted (equation 5) and estimated $\kappa_{AH_{coda}}$ values.

Often, Q_c is reported as a frequency-dependent parameter (*Aki and Chouet*, 1975, for the pioneering observations), thus one other important aspect of equation (5) is that it indicates a probable frequency dependence of $\kappa_{AH_{coda}}$. This was confirmed by our analysis, shown in Figure 5a; here, we plot the coda spectrum of the St.

Jean-de-Maurienne earthquake. It can be clearly observed that multiple lines (in different frequency bands) of varying slopes can be fit with the actual shape of the spectrum at high frequencies (> 8 Hz), irrespective of the components. It should also be noted that $\kappa_{AH_{coda}}$ decreases with frequency. A similar behavior is noteworthy for κ_{AH} measurements on the whole time series of the same event in Figure 5b. This again suggests a correlation between hard-rock κ_{AH} and $\kappa_{AH_{coda}}$; it also suggests that the classical frequency-independent κ model of *Anderson and Hough* (1984) is too simple to effectively describe the high frequency attenuation at hard-rock sites.

Conclusions

We used acceleration data recorded from crustal earthquakes that occurred in four different geological regions of France to discuss the interpretation of the well-known kappa value (*Anderson and Hough*, 1984). To achieve this goal, we benefited contiguous recordings of the same earthquake, obtained at rock and soil station sites in each of the four investigated areas. For each record, we performed two sets of κ measurements in the 16–32 Hz frequency band; one (i.e., κ_{AH}) was performed over the full time series, and the other (i.e., $\kappa_{AH_{coda}}$) was performed over the coda window of the same time series. We observed that $\kappa_{AH_{coda}}$ does not vary with soil type but shows significant regional variations. The latter are very well correlated with the regional variations of the coda quality factor Q_c. Essentially, this analysis shows that $\kappa_{AH_{coda}}$ can be used as a proxy to capture the regional hard-rock κ0ref that was pointed out by *Ktenidou et al.* (2015). From our theoretical analysis, we demonstrated that $\kappa_{AH_{coda}}$ estimated on the acceleration spectrum over a fixed frequency band (which is not classically performed) and Q_c estimated on the acceleration time series filtered in the same frequency band can be related to one another. This was further illustrated on data that the high-frequency shape (i.e., the slope of the linear trend) of the observed spectra is frequency dependent. In practice, this strong property is critical when performing HTTA for kappa in a seismic hazard assessment study. Indeed, it suggests that the common HTTA should depend on frequency. Because of the scarcity of data, further studies need to be addressed to statistically validate the robustness of the relation between (1) $\kappa_{AH_{coda}}$ and Q_c and (2) $\kappa_{AH_{coda}}$ and κ_{AH}. Nevertheless, we expect that this work will provide an opportunity for future studies to analyze the regional variations of the properties of coda waves and to take into account these variations for host-to-target GMPE adjustments.

Globally, the analysis presented in this article presents a new perspective for understanding the much-debated topic of kappa in engineering seismology. To achieve this, we used classical concepts and properties of coda waves widely used in physics-based seismological studies.

Data and Resources

The earthquake records used in this study were downloaded from the RESIF data center website (http://www.resif.fr, last accessed June 2017).

Acknowledgments

The authors acknowledge the RESIF group for the data distribution. RESIF is a National Research Infrastructure, recognized as such by the French Ministry of Higher Education and Research. RESIF is managed by the RESIF Consortium, which is composed of 18 research institutions and universities in France. Additionally, RESIF is supported by a public grant overseen by the French National Research Agency (ANR) as part of the Investissements d'Avenir program (reference: ANR-11-EQPX-0040) and the French Ministry of Environment, Energy and Sea.

References

Aki, K., and B. Chouet (1975). Origin of coda waves: Source, attenuation, and scattering effects, J. Geophys. Res. 80, no. 23, 3322–3342.

Anderson, J. G. (1991). A preliminary descriptive model for the distance dependence of the spectral decay parameter in southern California, Bull. Seismol. Soc. Am. 81, 2186–2193.

Anderson, J. G., and S. E. Hough (1984). A model for the shape of the Fourier amplitude spectrum of acceleration at high frequencies, Bull. Seismol. Soc. Am. 74, no. 5, 1969–1993.

Bora, S. S., F. Cotton, F. Scherbaum, B. Edwards, and P. Traversa (2017). Stochastic Source, Path and Site Attenuation parameters and associated variabilities for shallow crustal European earthquakes, Bull. Earthq. Eng. 15, no. 11, 4531–4561.

Bora, S. S., F. Scherbaum, N. Kuehn, P. J. Stafford, and B. Edwards (2015). Development of a response spectral ground motion prediction equation (GMPE) for seismic hazard analysis from empirical Fourier and duration models, Bull. Seismol. Soc. Am. 105, no. 4, 2192–2218.

Boore, D. M. (2003). Simulation of ground motion using the stochastic method, Pure Appl. Geophys. 160, no. 3, 635–676.

Brune, J. N. (1970). Tectonic stress and the spectra of seismic shear waves from earthquakes, J. Geophys. Res. 75, no. 26, 4997–5009.

Brune, J. N. (1971). Correction, J. Geophys. Res. 76, no. 20, 5002.

Calvet, M., and L. Margerin (2013). Lapse-time dependence of coda Q: Anisotropic multiple-scattering models and application to the Pyrenees, Bull. Seismol. Soc. Am. 103, no. 3, 1993–2010.

Calvet, M., M. Sylvander, L. Margerin, and A. Villaseñor (2013). Spatial variations of seismic attenuation and heterogeneity in the Pyrenees: Coda Q and peak delay time analysis, Tectonophysics 608, 428–439.

Campbell, K. W. (2003). Prediction of strong ground motion using the hybrid empirical method and its use in the development of ground-motion (attenuation) relations in eastern-north America, Bull. Seismol. Soc. Am. 93, no. 2, 1012–1033.

Carcolé, E., and H. Sato (2010). Spatial distribution of scattering loss and intrinsic absorption of short-period S waves in the lithosphere of Japan on the basis of the multiple lapse time window analysis of Hi-net data, Geophys. J. Int. 180, no. 1, 268–290.

Cotton, F., F. Scherbaum, J. J. Bommer, and H. Bungum (2006). Criteria for selecting and adjusting ground-motion models for specific target regions: Application to central Europe and rock sites, J. Seismol. 10, no. 2, 137–156.

Drouet, S., F. Cotton, and P. Gueguen (2010). VS30, κ, regional attenuation and Mw from accelerograms: Application to magnitude 3–5 French earthquakes, Geophys. J. Int. 182, no. 2, 880–898.

Edwards, B., O. Ktenidou, F. Cotton, N. Abrahamson, and C. Van Houtte (2015). Epistemic uncertainty and limitations of the k0 model for nearsurface attenuation at hard rock sites, Geophys. J. Int. 202, 1627–1645.

Edwards, B., C. Michel, P. Poggi, and D. Fäh (2013). Determination of site amplification from regional seismicity: Application to the Swiss National Seismic Network, Seismol. Res. Lett. 84, no. 4, 611–621.

Hanks, T. C. (1982). Reply to "Comments on 'The corner frequency shift, earthquake source models, and Q'", Bull. Seismol. Soc. Am. 72, no. 4, 1433–1444.

Kilb, D., G. Biasi, J. Anderson, J. Brune, Z. Peng, and F. L. Vernon (2012). A comparison of spectral parameter kappa from small and moderate earthquakes using southern California Anza seismic network data, Bull. Seismol. Soc. Am. 102, no. 1, 284–300.

Ktenidou, O., N. Abrahamson, S. Drouet, and F. Cotton (2015). Understanding the physics of kappa (κ): Insights from a down-hole array, Geophys. J. Int. 203, no. 1, 678–691.

Ktenidou, O., F. Cotton, N. Abrahamson, and J. Anderson (2014). Taxonomy of κ: A review of definitions and estimation approaches targeted to applications, Seismol. Res. Lett. 85, no. 1, 135–146.

Ktenidou, O., S. Drouet, N. Theodulidis, M. Chaljub, S. Arnaouti, and F. Cotton (2012). Estimation of kappa (κ) for a sedimentary basin in Greece (Euroseistest): Correlation to site characterization parameters, Proc., 15th World Conf. of Earthquake Engineering, Lisbon, Portugal, 24–28 September 2012.

Lacombe, C., M. Campillo, A. Paul, and L. Margerin (2003). Separation of intrinsic absorption and scattering attenuation from Lg coda decay in central France using acoustic radiative transfer theory, Geophys. J. Int. 154, no. 2, 417–425.

Lai, T. S., H. Mittal, W. A. Chao, and Y. M. Wu (2016). A study on kappa value in Taiwan using borehole and surface seismic array, Bull. Seismol. Soc. Am. 106, no. 4, 1509–1517.

Leary, P., and R. Abercrombie (1994). Frequency dependent crustal scattering and absorption at 5–160 Hz from coda decay observed at 2.5 km depth, J. Geophys. Res. 21, no. 11, 971–974.

Mayor, J., M. Calvet, L. Margerin, O. Vanderhaeghe, and P. Traversa (2016). Crustal structure of the Alps as seen by attenuation tomography, Earth Planet. Sci. Lett. 439, 71–80.

Mayor, J., L. Margerin, and M. Calvet (2014). Sensitivity of coda waves to spatial variations of absorption and scattering: Radiative transfer theory and 2-D examples, Geophys. J. Int. 197, no. 2, 1117–1137.

Mayor, J., P. Traversa, M. Calvet, and L. Margerin (2017). Tomography of crustal seismic attenuation in Metropolitan France: Implications for seismicity analysis, Bull. Earthq. Eng. 1–16.

Molkenthin, C., F. Scherbaum, A. Griewank, H. Leovey, S. Kucherenko, and F. Cotton (2017). Derivative-based global sensitivity analysis: Upper bounding of sensitivities in seismic-hazard assessment using automatic differentiation, Bull. Seismol. Soc. Am. 107, no. 2, 984, doi:

10.1785/0120160185.
Paul, A., S. Gupta, and C. C. Pant (2003). Coda Q estimates for Kumaun Himalaya, J. Earth Syst. Sci. 112, no. 4, 569–576.
Rautian, T., and V. Khalturin (1978). The use of the coda for determination of the earthquake source spectrum, Bull. Seismol. Soc. Am. 68, no. 4, 923–948.
Renault, P. (2014). Approach and challenges for the seismic hazard assessment of nuclear power plants: The Swiss experience, Boll. Geof. Teor. Appl. 55, no. 1, 149–164.
Rodriguez-Marek, A., E. M. Rathje, J. J. Bommer, F. Scherbaum, and P. J. Stafford (2014). Application of single-station sigma and site-response characterization in a probabilistic seismic-hazard analysis for a new nuclear site, Bull. Seismol. Soc. Am. 104, no. 4, 1601–1619.
Sato, H., and M. C. Fehler (2007). Synthesis of seismogram envelopes in heterogeneous media, Adv. Geophys. 48, 561–596.
Sato, H., M. C. Fehler, and T. Maeda (2012). Seismic Wave Propagation and Scattering in the Heterogeneous Earth, Springer, 496 pp.
Sedaghati, F., and S. Pezeshk (2016). Estimation of the coda-wave attenuation and geometrical spreading in the New Madrid Seismic Zone, Bull. Seismol. Soc. Am. 106, 1482–1498, doi: 10.1785/ 0120150346.
Steensma, G., and N. Biswas (1988). Frequency dependent characteristics of coda wave quality factor in central and south-central Alaska, in Scattering and Attenuations of Seismic Waves, Part I, Springer, 295–307.
Van-Houtte, C., S. Drouet, and F. Cotton (2011). Analysis of the origins of κ (kappa) to compute hard rock to rock adjustment factors for GMPEs, Bull. Seismol. Soc. Am. 101, no. 6, 2926–2941.
Zandieh, A., K. W. Campbell, and S. Pezeshk (2016). Estimation of κ0 implied by the high-frequency shape of the NGA-West2 ground-motion prediction equations, Bull. Seismol. Soc. Am. 106, 1342–1356, doi: 10.1785/0120150356.

GFZ German Research Center for Geosciences
Helmholtzstraße 6/7
14467 Potsdam
Germany
sanjay.bora@sed.ethz.ch